DESIGN OF A SUPERCONDUCTING SOLENOID SUITABLE TO WORK WITH A LASER PARTICLE SOURCE

CERN Summer Student Programme 2021 Report

Supervisors: Kenneth Long, Colin Whyte, Josef Boehm

Student: Alejna Beqiri

Participation Period: July 05 – August 27, 2021

Abstract

The main objective of the CERN Summer Student Project was to design a superconducting solenoid, which is suitable to use in a custom installation for the capture of protons, emitted from a thin foil target and illuminated by a high power short pulse laser. The magnet must not interfere with the laser delivery system or its vacuum chamber. For this reason, changes from a conventional superconducting magnet design were required. The superconducting coil will be cooled using a cryogen-free system. This report presents the magnetic and thermal analysis of the solenoid. Two different magnetic models and four thermal models were designed using the FEMM software. The overall goal of the project to design a superconducting solenoid that meets the required characteristics to operate within a space restricted apparatus was achieved.

Contents

1. Introduction

A pair of superconducting solenoids were proposed to be used at the LhARA project [1] to capture the divergent flux of protons arising from the laser target. In this project it is presented a first design for the first of the two superconducting solenoids.

The solenoid should be 1 m long and it should have a warm bore of 60 mm in diameter. Inside the warm bore of the magnet, the produced magnetic field should be 1.3 T. A vacuum tube will be inserted into the warm bore, which will be used to capture and focus the proton beam. The magnetic field at the target should be less than 50 mT.

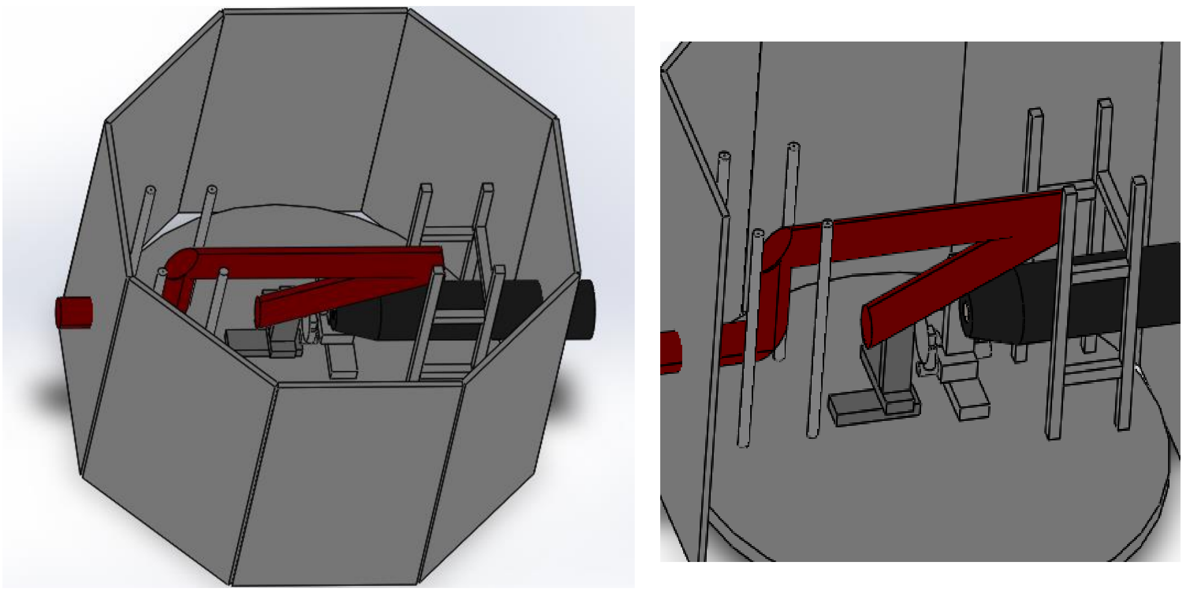

Figure 1 – Simplified CAD Model from Colin Whyte

Figure 1 shows a simplified CAD Model in which the main components of the overall system are presented. The octagon is the vacuum vessel, while the round plate where all the parts sit on is called the breadboard. The laser beam (in red) is brought into the vacuum vessel from one side and it is focused on the thin foil target. The magnet should be inserted from the opposite side and positioned at the back of the target.

The outer diameter of the magnet envelope was initially proposed to be 300 mm. However, the space where one can put the magnet is constrained, because it must not interfere with the laser delivery system or its vacuum chamber. A possible option was to make the input end of the magnet as small physically as possible, so it will not get on the way of anything else.

The idea is that the closer one can get the solenoid to the source the better, because closer to the magnet the beam is smaller, diverging from a point source at an angle of a few degrees. In order to minimize the distance between the magnet and the target, the input end of the magnet was tapered in form of a “sharpened pencil’’.

Figure 2 shows how close the magnet envelope approaches the laser beam with an input end of 150 mm OD and 60 mm ID for the vacuum bore. With an outer diameter of 150 mm, the closest position that the magnet can get to the target is about 150 mm.

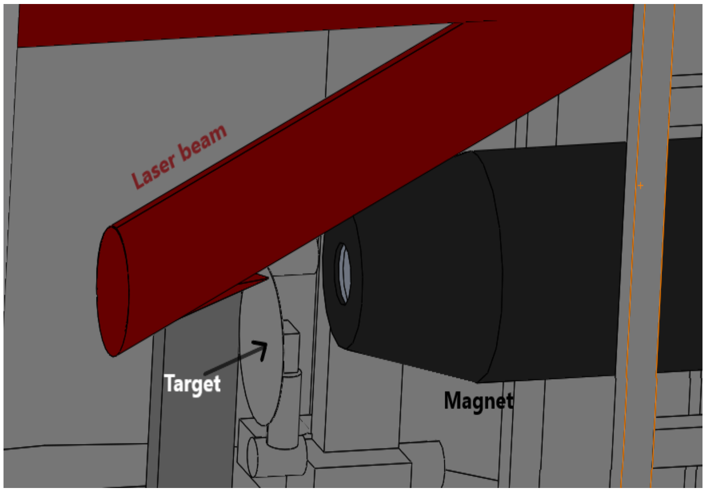

Figure 2 – Minimum distance between the magnet and the target

The cross-section of the magnet with all its components it is shown in Figure 3. Each component and its function will be discussed later on.

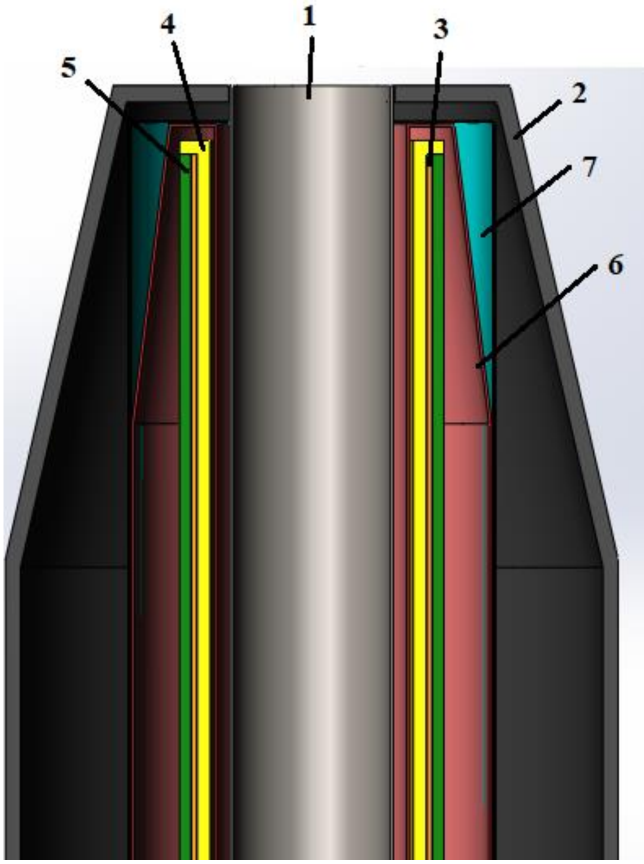

1	Vacuum Tube
2	Vacuum Envelope
3	Coil
4	Former
5	Heat Shunt
6	Radiation Shield
7	Superinsulation - MLI

Figure 3 - Main components of the magnet

2. Requirements for the superconducting coil

Superconducting magnetic coils have the capability of generating extremely powerful magnetic fields with no, or negligible, electrical resistivity below a critical temperature, T_C. They enable the construction of powerful magnetic fields which are not constrained by the high power requirements and resistance losses associated with standard electromagnets. Superconducting materials are classified in two general categories: Low Temperature Superconductors (LTS), with a T_C less than ~35 K, and High Temperature Superconductor (HTS), with T_C values of up to ~100K. LTS magnets are typically operated in the range of 4.2 K, the boiling point of liquid helium.

The coil assumed to be used in this magnet is a Niobium-Titanium alloy, which is a Low Temperature Superconductor (LTS). Its critical temperature is 9.2 K. Nb-Ti alloy is currently the standard 'work horse' of the superconducting magnet industry. It is a ductile alloy with mechanical properties which make it easy to fabricate and use [2]. It has been used in the majority of the accelerators so far constructed or planned, for MRI systems and most other magnets.

During its operation, the coil must be cooled below 5 K because the lower the temperature, the higher the currents and magnetic fields it can stand without returning to its resistive state. The most convenient way to cool this magnet is through cryogen-free system.

2.1. Cryogen - free system

A cryogen-free system is one that provides cryogenic cooling without the consumption of cryogenic liquids such as liquid nitrogen or liquid helium. Cooling of cryogen-free systems is done by cryo-coolers, also known as cold heads. Usually the cryo-coolers use a cryogenic fluid as the working substance and use moving parts to cycle the fluid around a thermodynamic cycle, such that the fluid will not be consumed. Cryocoolers lower the temperature basically through compression and expansion of a working fluid, normally Helium, and there are a number of types that vary in the cooling cycles and the principles used.

Figure 4 – RDK408D2 4K cryo-cooler from SHI Cryogenics

A two-stage GM cryocooler will be used for this magnet (Figure 4). The cryocooler should have a power of 1 W at 4 K stage and 40 W at 50 K stage. More informations about these systems can be found from different suppliers.

3. Magnetic field of the solenoid

Solenoids are commonly used in many applications as a way to create a uniform magnetic field, which means having a constant magnetic field in some region of space. An ideal solenoid is considered one that has the radius of its coils very small compared to its overall length and has its coils closely spaced together. The field is concentrated in the interior of the coil and is considerably weaker outside the coil. An infinitely long coil will have zero field outside. For a real solenoid, however, magnetic field is not constant because it drops to half of the magnitude at the ends and some field exists outside the solenoid.

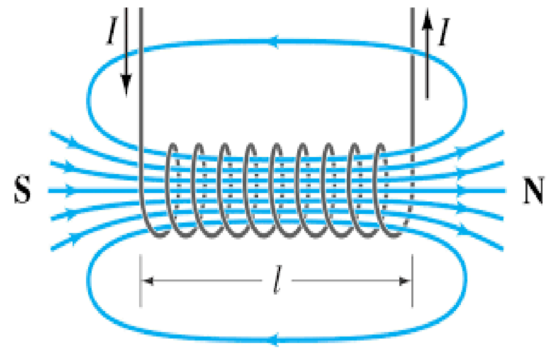

Figure 5 - Magnetic field of a solenoid

The magnetic field inside an ideal solenoid with number of turns N, length L, and current I may be calculated from Ampere's law and has magnitude of:

$$B = \mu_0 \frac{N}{l} \mathrm{I} \quad (1)$$

where μ_0 is the permeability of free space with value $4\pi \times 10^{-7}$ Tm/A .

In this project the goal is to design a 1m long solenoid which produces 1.3 T field for a current of 250 A. So, for the number of turns of the coil using the Ampere's law one gets:

$$N = \frac{B \cdot l}{\mu_0 \cdot I} = \frac{1.3 \cdot 1}{4\pi \cdot 10^{-7} \cdot 250} \quad (2)$$

N = 4140 turns

Because of the complex structure, one can no longer rely only on simple analitycal calculations for the design of modern magnets. In order to determine the electromagnetic structure parameters of the magnet, different numerical analysis have been developed.

3.1 . Finite Element Method Magnetics (FEMM)

FEMM is a suite of programs for solving low frequency electromagnetic problems on two-dimensional planar and axi-symmetric domains. The program currently addresses linear/nonlinear magnetostatic problems, linear/nonlinear time harmonic magnetic problems, linear electrostatic problems, and steady-state heat flow problems [3].

3.2 . Models of the magnetic field

Two axi-symmetrical models of the solenoid have been created using the FEMM software. The models have been simplified in the sense that, some of the geometries are not detailed because we do not need them for the magnetics analysis.

In the first model, there is drawn only the cold mass composed of the superconducting coil, the former and the heat shunt (Figure 6). As material for the former and the heat shunt was chosen Aluminium 1100 because of its high thermal conductivity. The coil has an inner diameter of 87 mm, an outer diameter of 91 mm and an axial length of 1000 mm. Instead of using a single layer coil, in this project a two-layer coil with about 2070 turns per layer will be used. A current of 250 A was considered to flow through the coil. Because it is an axi-symmetric model, it is enough to

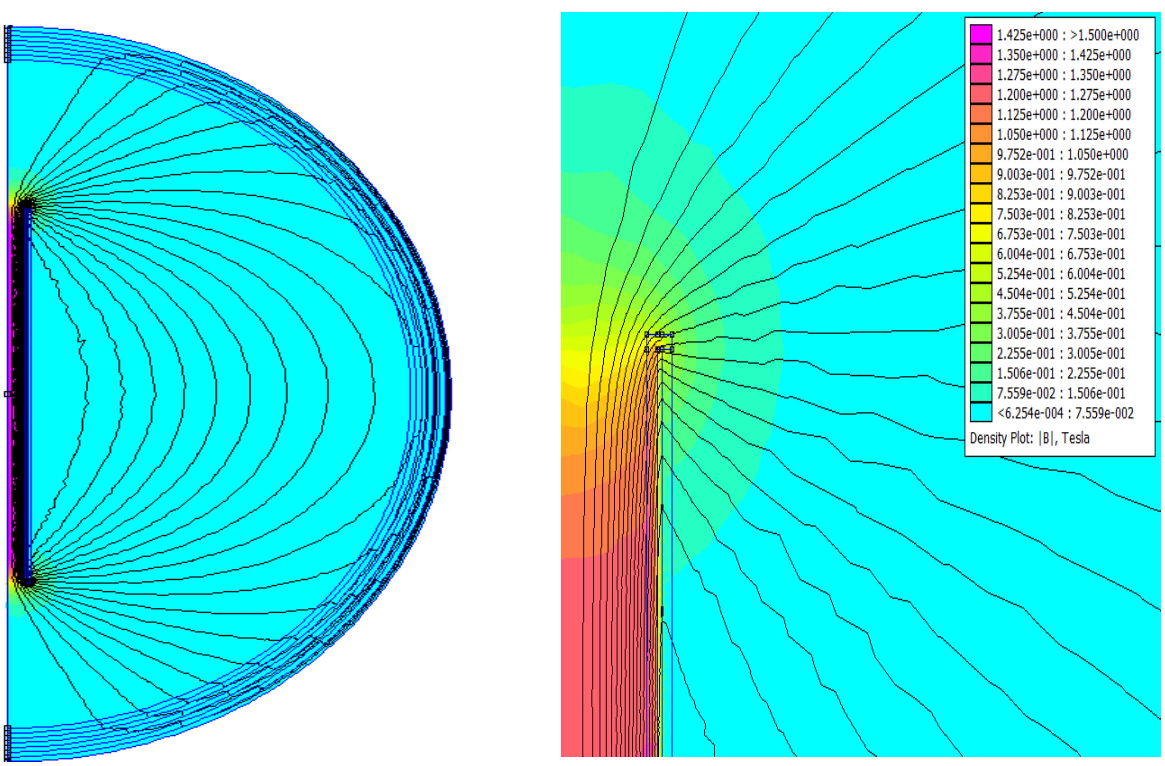

Figure 6 – Simulation of the magnetic field density of the cold mass

model just half of it. The model is drawn vertically, with r-axis lying horizontally and z-axis vertically. It is centred around the point r=0, z=500mm and then Dirichlet boundary conditions are drawn around it.

The magnetic field which is formed inside the warm bore is around 1.3 T, but the problem in this model is with the stray field on the outside which could interfere with other components of the system. This was the reason for an iron "jacket" around the magnet.

Adding an iron shield around the cold mass was necessary to limit the magnetic field outside the magnet bore. Actually, the iron shield represents the vacuum envelope of the magnet. The preferred material for the vacuum envelope was chosen to be 1010 carbon steel, which is a plain carbon steel with 0.10% carbon content. The steel is thinner at the tip of the input end, but it becomes thicker where the walls are cylindrical with a thickness of 10mm.

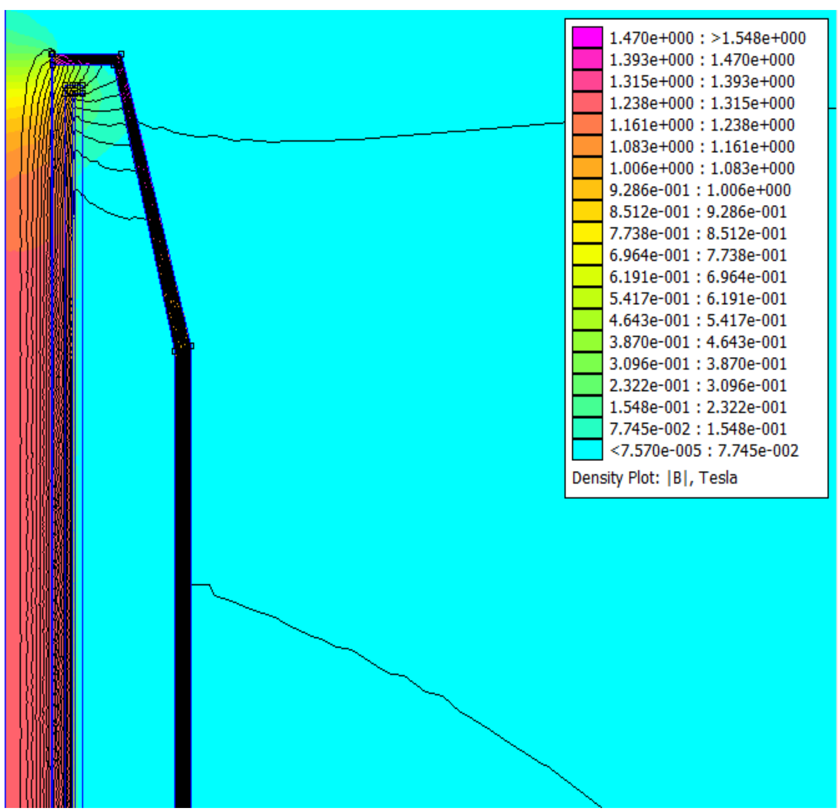

Figure 7 – Simulation of the magnetic field density with the iron shield

As it can be seen from the simulation of the model in Figure 7 and the plot of the magnetic field density in Figure 8, inside the bore there is a field of 1.3 T and then at both ends of the magnet the field drops to around 0.5 T, but the stray field from the unit is very low. The iron shield was made thicker in order to allow it to carry the entire return flux. According to this model, the stray field at the target would be very low - around 2.6 mT.

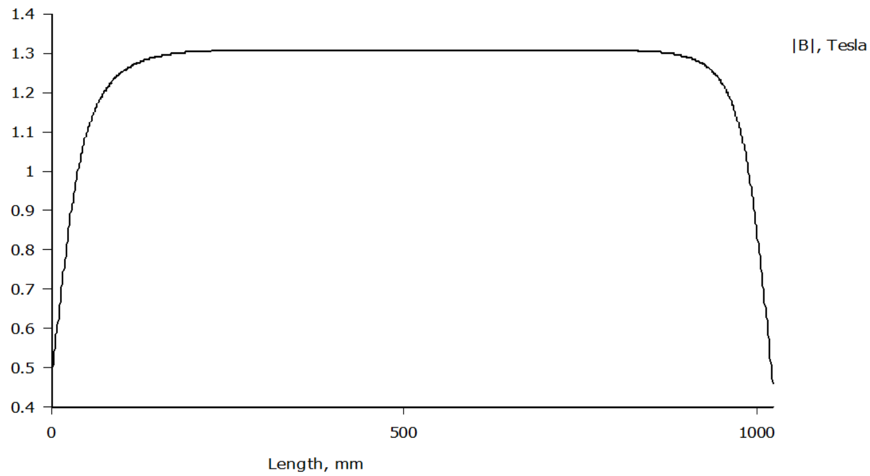

Figure 8 – Plot of the magnetic field flux density along the axis of the magnet

Much informations about the coil are shown in the table below:

Coil length [mm]	1000
Coil inner radius [mm]	38.5
Coil thickness [mm]	0.5
Winding bed [mm]	2
Number of layers	2
Number of turns per layer	2070
Cross – section of the coil [m^2]	0.002
Coil current [A]	250
Current density [MA/m^2]	502.513

Table 1 – Coil parameters

4. Thermal model

4.1. Analytical calculations

One of the key issues for the normal operation and safety of the magnet system is the thermal stability. The heat load assumed in this magnet system includes:

- conduction through the magnet supports and current leads;
- radiation of heat coming from the outer environment which is at room temperature (300K) and heating the 4K components inside the cryostat.

Convection is not considered here because the space inside the cryostat is vacuum.

Thermal radiation is further reduced by the use of a radiation shield and by superinsulation, also called MLI (multi-layer insulation). The radiation shield is connected to the first stage of the cold head and it is cooled to around 50 K, meanwhile the cold mass is connected to the second stage and it is cooled to 4 K. Radiation is related to the temperature to the power 4, so without the radiation shield there would be a very high radiative heat load falling onto the cold mass.

By using some layers of MLI around the radiation shield there is only a heat load of about 1-1.5 W/m^2 falling onto the radiation shield. Usually there is no need for an extra layer of MLI between the radiation shield and the cold mass, so there will be only thermal radiation between the two surfaces, and the heat load can easily be calculated using the following equation [4]:

$$q = F\sigma(T_2^4 - T_1^4) = \frac{0.1}{2} \cdot 5.6704 \cdot 10^{-8} \cdot (50^4 - 4^4) \qquad (3)$$

$$q = 0.0177\ [W/m2]$$

where F is the geometry factor between two concetric surfaces and σ is the Stefan – Boltzmann constant. So, the overall radiative heat load is low and it can be handled by the cryo-cooler.

The biggest heat input onto the systemm will come from the conduction of the copper current leads. One has to optimise the current leads such as: the resistivity must be low and the conductivity must be low as well. There are programs and methods that optimise the current leads in order to minimise the heat input.

Analitycal calculations can be made for the current leads as well. The first two copper leads from 300 K are connected to the first stage of the cryocooler. If we assume that the current which flows through the wires is 300 A and the wire is 200 mm in length and 5 mm in diameter than we can calculate both the power dissipated (Joule heat) and the power conducted per wire:

- The electrial resistance of the wire and the power dissipated:
  $\rho_{Cu}(100K) = 3{,}5 \cdot 10^{-9}\ [\Omega/m]$
  - $R_e = \rho \frac{L}{A} = 3.5 \cdot 10^{-9} \frac{0.2}{196 \cdot 10^{-7}} = 0.00003571\ [\Omega]$ (4)
  - $P = I^2 R = 300^2 \cdot 0.00003571 = 3.21\ [W]$ (5)
- The thermal resistance of the wire and the power conducted/heat load:

$k_{Cu}(100K) \approx 440[W/mK]$

- $R_t = \frac{L}{kA} = \frac{0.2}{440 \cdot 196 \cdot 10^{-7}} = 25.5\ [K/W]$ (6)
- $Q = -dT\frac{1}{R_t} = \frac{300-50}{25.5} = 9.8\ [W]$ (7)

Then we can repeat the calculations for the additional HTS leads that go from 50 K down to 4 K, but because we have a superconductor the electrical losses will be zero. For the HTS leads we can use a wire which is 200 mm in length and 0.5 mm in diameter.

- $R_e = 0;\ P = 0;$
- The thermal resistance of the wire and the power conducted/heat load:

$k = 1250[W/mK]$

- $R_t = \frac{L}{kA} = \frac{0.2}{1250 \cdot 0.000000196} = 816.33\ \left[\frac{K}{W}\right]$ (9)
- $Q = -dT\frac{1}{R_t} = \frac{50-4}{816.33} = 0.056[W] = 56\ [mW]$ (10)

What can be concluded from these calculations is that for the current leads going from 300 K to 50 K one would have about 6.5 W power dissipated through both wires and about 19.6 W power conducted. So, the total heat load would be around 26 W from both wires. Knowing that the cooling capacity of the cold head at 50 K is around 40 W, it means that the resulted heat load would be manageable from the cold head. Also, the heat load from the HTS leads is very small, so it would be affordable by the cold head which at 4 K stage has a power of 1 W.

4.2. FEMM models

In the thermal analysis, four different 2D axisymmetric models of the solenoid have been developed. Some assumptions have been made in the models such as: the cross-sections of each stage of the cryocooler are regarded as square ones and the heat loads from the support structures for the cold mass and radiation shield are not considered.

4.2.1. First model – Cold head connected to the bottom of the cold mass

On the first developed model, both stages of the cryo-cooler were connected to the bottom end of the cold mass and radiation shield respectively, which is the usual arrangement in practice (Figure 9). The boundary conditions on the model were:

- Fixed temperature of 50 K at the bottom surface of the first stage of the cold head
- Fixed temperature of 4 K at the bottom surface of the second stage of the cold head
- The outer boundaries of the vacuum envelope defined as 300 K room temperature

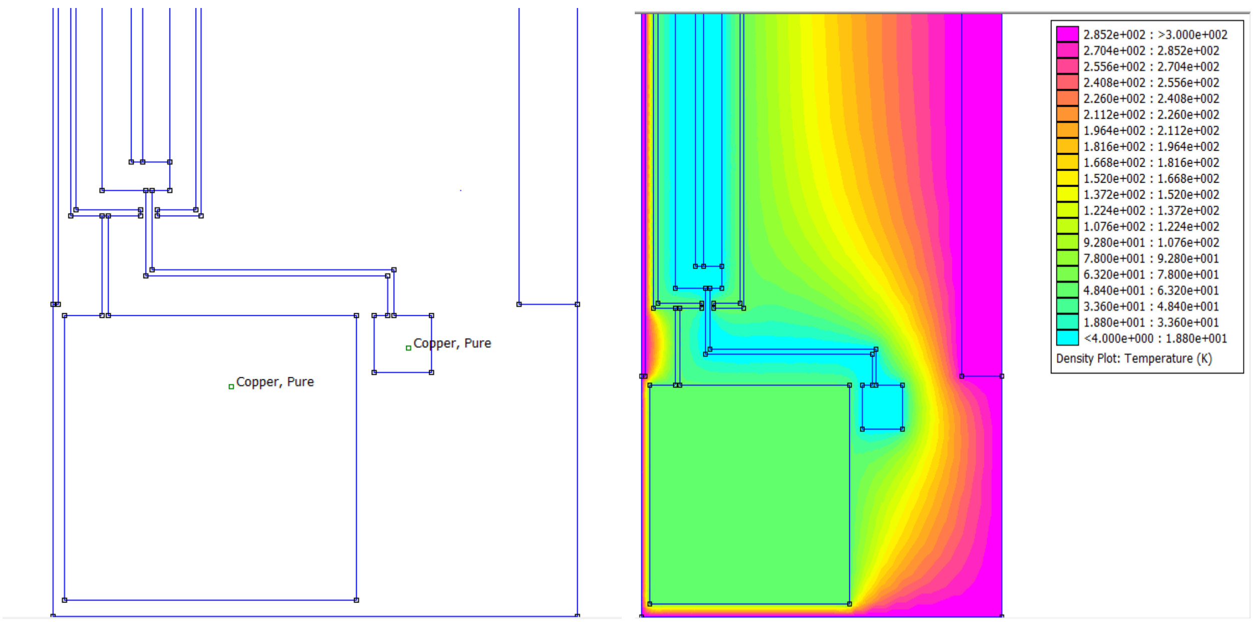

Figure 9 - Simulation of the first thermal model

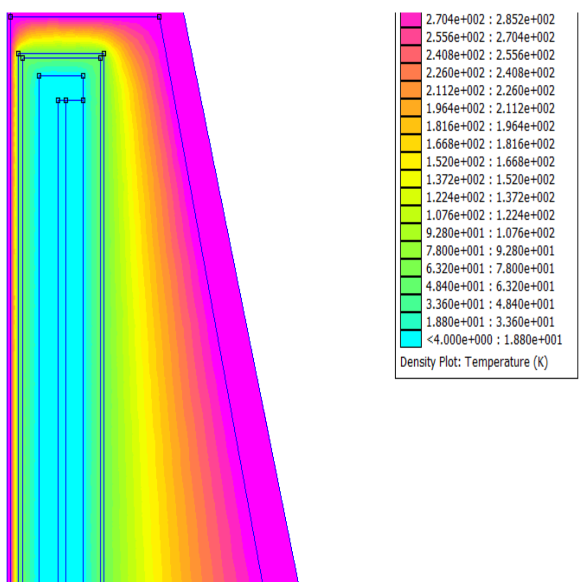

Figure 10 - Upper part of the simulation

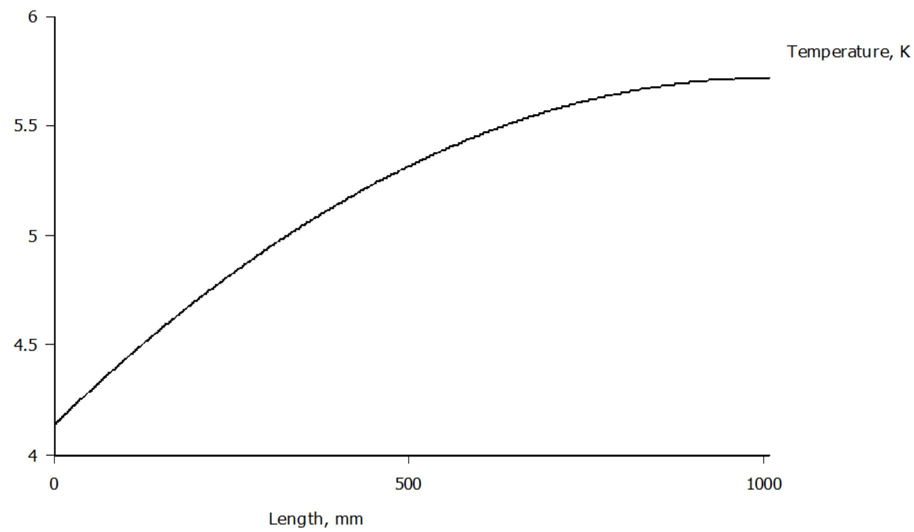

Figure 11 – Temperature distribution along the cold mass

But the results for the temperature distribution along the cold mass were not very satisfying. At the tip of the cold mass the temperature increased up to 5.7 K (Figure 11). If the cold mass achieves that temperature at the tip that would mean that the coil could retrieve its resistivity and lose the superconductivity.

4.2.2. Second model – Cold head connected horizontally

Another way to insert the cold head is horizontally, such that the cold head is parallel to the cold mass and 400 mm from its bottom, which puts the 4 K stage quite close to the middle of the cold mass (Figure 12). Usually it is not preferred to have the cold head in a horizontal position because it can lose its full cooling capacity, but in this case it gives a better temperature distribution along the cold mass. Also, the cross-section of the 50 K stage was reduced because that does not affect the results. Again the same boundary conditions were defined.

As it can be seen from the graph in Figure 13, the cold mass has the lowest temperature at the place where it is connected to the 4 K stage which is in a distance of 400 mm from the very bottom and then it has a temperature of around 4.5 K at the bottom end and 4.8 K at the top. But the temperature on the radiation shield was very high in this model, so it was necessary somehow to include into the model the fact that there will be some layers of MLI between the radiation shield and the vacuum envelope.

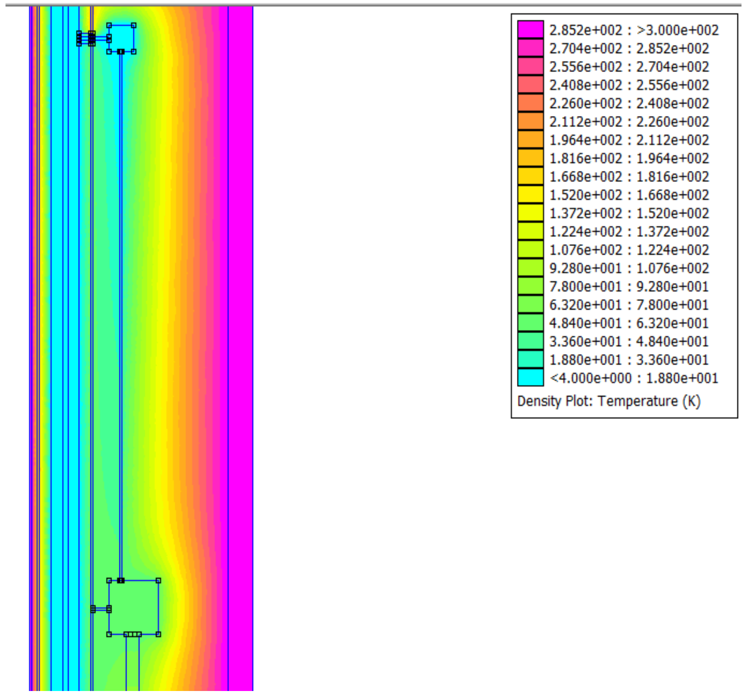

Figure 12 - Simulation of the second thermal model

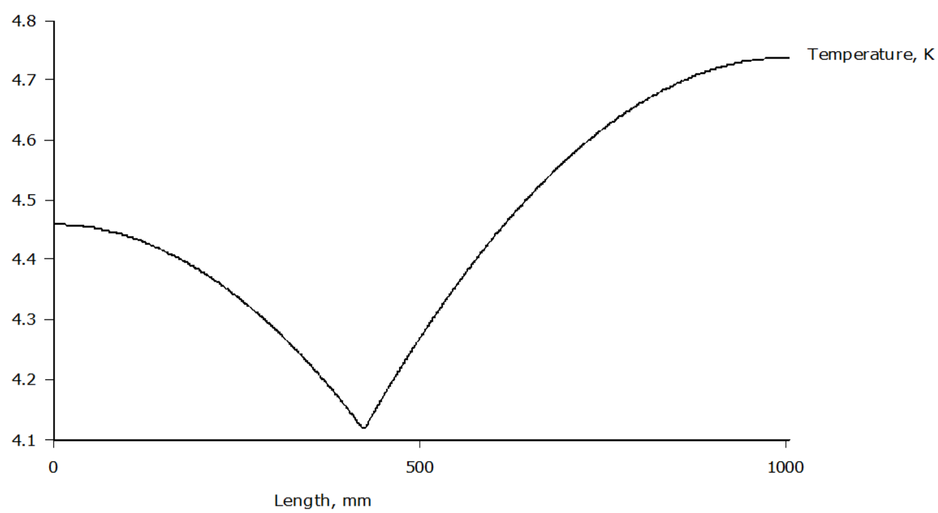

Figure 13 – Temperature distribution along the cold mass

4.2.3. Third model – Using heat flux boundaries and moving the 4K stage and HTS leads inside the radiation shield

Except from defining a boundary as a fixed temperature, FEMM includes the possibility to define a boundary as a heat flux. So, in this model the outer boundaries of the vacuum envelope were defined as heat flux boundaries because in that way one could approximate what would actually happen with the superinsulation. Now, the outer boundaries are set as a heat flux of 1.5 W/m2, except from the bottom bounday which is set at a fixed temperture of 300 K because of the copper current leads. Also, the second stage of the cold head together with the HTS leads are placed into the vacuum space between the cold mass and the radiation shield.

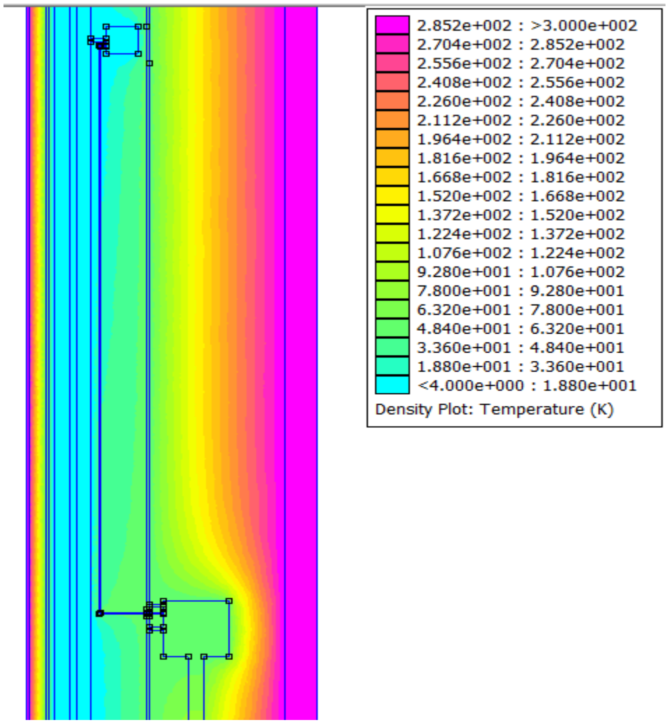

Figure 14 - Simulation of the third thermal model

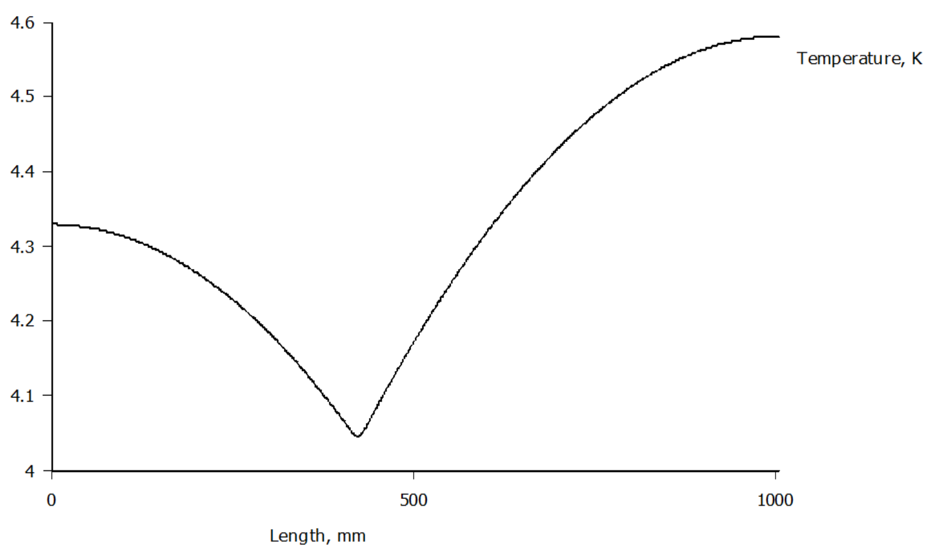

Figure 15 - Temperature distribution along the cold mass

In this model the highest temperature on the radiation shield is around 54 K. Also, the temperature slightly dropped on both ends of the cold mass (Figure 15).

4.2.4. Last model – Applying the 'sharpened pencil' form to the radiation shield

The last change on the model was to change the form of the radiation shield at the top and make it like a sharpened pencil form, similar to the iron shield. In this way, less heat load will be concentrated at the tip of the shield.

Another important reason for this change was due to the insufficient place for the superinsulation. Actually, at the warm bore side there is still not much place left for the superinsulation, but one could manage to put there 5-10 layers of MLI.

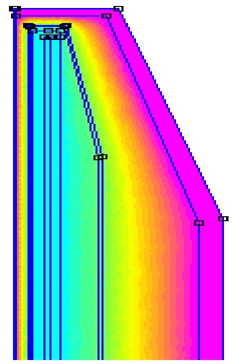

Figure 16- Adjusting the form of the shield

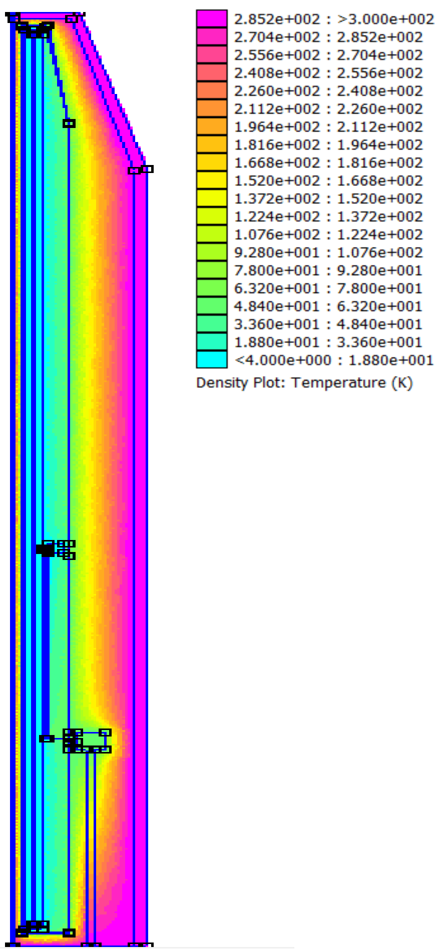

Figure 17- Simulation of the last thermal model (full model)

MLI is a key component in the reduction of heat leak to cryogenic systems due to thermal radiation. Most MLI systems consist of thin reflective layers separated from each other by thermally insulating layers. These layers of MLI help to drastically reduce the heat load falling onto radiation shield to a value of 1 to 1,5 W/m^2.

As material for MLI, one could use electro-polished aluminium or copper because of the low emissivity. Increasing the number of layers and decreasing the emissivity both lower the heat load, which is equivalent to a better achieved superinsulation.

As it can be seen from the last simulation, with this model better results were achieved.

5. Conclusion

A 2D axi-symmetric model of a superconducting solenoid with the required characteristics to fit into a space constrained installation was developed.

Using FEMM software the magnetic field profile of the solenoid was modelled. The main requirement of 1.3 T magnetic field inside the bore of the magnet was achieved. However, an iron shield around the cold mass was added to reduce the stray field outside the magnet to ensure that it will not interfere with other components of the overall system.

Different methods were used to design the thermal model of the solenoid. The last developed thermal model of the solenoid system was used to show that the magnet can achieve the temperatures required for superconducting operation when a cryo-cooler with 1 W capacity at 4 K and 40 W capacity at 50 K is used.

Having in consideration the fact that FEMM software supports only 2D modelling, there are some limitations in both the magnetic and thermal models. So, these results are more like an approximation of what one would have in pratice.

Because of the deadline of the project there was not enough time to analyse the mechanical aspect of the solenoid. The radiation shield and the cold mass need to be supported mechanically within the cryostat. That will add 10 to 50 mW extra heat into the system. For these structures one can use non-metallic structures like G10 material which is a high pressure fibre-glass laminate. These structures should be designed carefully as they may add more heat into the system.

Considering the results from the simulations, it can be concluded that the main goal of the project to design a superconducting solenoid that meets the required conditions to operate within a space restricted installation was achieved.

6. Acknowledgements

I would like to express my sincere gratitude to my supervisors Dr. Kenneth Long, Dr. Colin Whyte and Dr. Josef Boehm, for the clear guidance and helpful suggestions in every step of the way going through with this project. Their contribution and encouragement helped me learn and explore new things, while at the same time enjoying my virtual summer with CERN. I am thankful to CERN Summer Student Programme for giving me this opportunity and “The three physicists” foundation for funding my participation as a CERN Non-Member State student. Also, many thanks to Rebecca Louise Taylor for helping me with every uncertainty during the programme.

References

[1] G.Aymar, T. Becker, S. Boogert, M. Borghesi, R. Bingham, C. Brenner, … & R. Xiao. "*LhARA: the laser-hybrid accelerator for radiobiological applications*", (2020). https://dx.doi.org/10.3389/fphy.2020.567738

[2] M. N. Wilson, "*Superconducting materials for magnets*", (1996). DOI: 10.1002/9783527670635.ch4

[3] D. Meeker, "*Finite Element Method Magnetics Software*", (2015). http://www.femm.info/Archives/doc/manual42.pdf

[4] B. A. Hands, "*Cryogenic Engineering*" (1986), pp. 107-112.